by the temperature change of a few degrees near T_c of the liquid crystal. The viscosity of the nematic phase of EBBA is in the same range as that of liquid water, and the liquid-crystalline domain supposedly acts as the efficient mobile region of the gases. It was concluded by these authors that the temperature dependence of P is influenced by the thermal motion of the membrane component as well as by the continuity and/or size of the liquid-crystal phase.

An analogous argument may be presented for interpretation of the permeation characteristics of the multicomponent bilayer film. Discontinuous jump of P at T_c is ascribable to greater gas mobility in the liquid-crystalline phase of the hydrocarbon component, and the jump becomes larger as the hydrocarbon domain is enlarged.

Concluding Remarks

Multicomponent bilayer membranes can be immobilized in the form of PVA composite films. The DSC and XPS data indicate that the hydrocarbon and fluorocarbon bilayer components are phase-separated and that the fluorocarbon component is concentrated near the film surface. These component distributions produce favorable effects on permselectivity of O_2 gas. The selectivity (P_{O_2}/P_{N_2}) is apparently determined by the surface monolayer (or layers close to the surface) of the fluorocarbon component, and the permeability is promoted by the presence of large domains of the fluid (in the liquid-crystalline state) hydrocarbon bilayer.

Acknowledgment. We extend our appreciation to the Asahi Glass Foundation for Industrial Technology for financial support.

Registry No. 1, 91362-66-2; 2, 89373-65-9; 3, 100993-84-8; 4, 100993-85-9; 5, 82838-66-2; O_2, 7782-44-7; N_2, 7727-37-9.

References and Notes

(1) Nakashima, N.; Ando, R.; Kunitake, T. *Chem. Lett.* **1983**, 1577.
(2) Shimomura, M.; Kunitake, T. *Polym. J. (Tokyo)* **1984**, *16*, 187.
(3) Higashi, N.; Kunitake, T. *Polym. J. (Tokyo)* **1984**, *16*, 583.
(4) Kunitake, T.; Tsuge, A.; Nakashima, N. *Chem. Lett.* **1984**, 1783.
(5) Kunitake, T.; Higashi, N.; Kajiyama, T. *Chem. Lett.* **1984**, 717.
(6) Takahara, A.; Kajiyama, T., personal communication.
(7) Kunitake, T.; Tawaki, S.; Nakashima, N. *Bull. Chem. Soc. Jpn.* **1983**, *56*, 3235.
(8) Kunitake, T.; Higashi, N. *J. Am. Chem. Soc.* **1985**, *107*, 692.
(9) Kunitake, T.; Asakuma, S.; Higashi, N.; Nakashima, N. *Rep. Asahi Glass Found. Ind. Technol.* **1984**, *45*, 163.
(10) Okahata, Y.; Ando, R.; Kunitake, T. *Ber. Bunsen-Ges. Phys. Chem.* **1981**, *85*, 789.
(11) Barrer, R. M.; Skirrow, G. *J. Polym. Sci.* **1948**, *3*, 549.
(12) Hoffman, S. "Depth Profiling" in *Practical Surface Analysis*; Briggs, D.; Seak, M. P., Eds.; Wiley: New York, 1983.
(13) Brundle, C. R. *J. Vac. Sci. Technol.* **1974**, *11*, 212.
(14) Kajiyama, T.; Nagata, Y.; Washizu, S.; Takayanagi, M. *J. Membr. Sci.* **1982**, *11*, 39.
(15) Kajiyama, T.; Washizu, S.; Takayanagi, M. *J. Appl. Polym. Sci.* **1984**, *29*, 3955.
(16) Washizu, S.; Terada, I.; Kajiyama, T.; Takayanagi, M. *Polym. J. (Tokyo)* **1984**, *16*, 307.
(17) Kajiyama, T.; Washizu, S.; Ohmori, Y. *J. Membr. Sci.* **1985**, *24*, 73.

Phase Equilibria in Rodlike Systems with Flexible Side Chains†

M. Ballauff

Max-Planck-Institut für Polymerforschung, 65 Mainz, FRG. *Received July 31, 1985*

ABSTRACT: The lattice theory of the nematic state as given by Flory is extended to systems of rigid rods of axial ratio x and appended side chains characterized by the product of z, the number of side chains per rod, and m, the number of segments per side chain. Soft intermolecular forces are included by using the familiar interaction parameter. Special attention is paid to the form of the orientational distribution function, which is introduced in terms of the refined treatment devised by Flory and Ronca as well as in its approximative form given by Flory in 1956. At nearly athermal conditions the theory presented herein predicts a narrowing of the biphasic gap with increasing volume fraction of the side chains. The region where two anisotropic phases may coexist becomes very small in the presence of side chains. It is expected to vanish at a certain critical volume ratio of side chains and rigid core of the polymer molecule. The dense anisotropic phase at equilibrium with a dilute isotropic phase at strong interactions between the solute particles (wide biphasic region) is predicted to become less concentrated with increase of the product of z and m. The deductions of the treatment presented herein compare favorably with results obtained on lyotropic solutions of helical polypeptides like poly(γ-benzyl glutamate).

During recent years there has been a steadily growing interest in thermotropic and lyotropic polymers. Spinning or injection molding in the liquid-crystalline state can lead to fibers of high strength and stiffness.[1] However, the melting point of typical aromatic polyesters exhibiting a mesophase often exceeds 500 °C,[2] which makes the processing of these materials by conventional methods very difficult. In order to reduce the melting temperature of thermotropic polymers, flexible spacers have been inserted between the mesogenic units.[3] But these semiflexible polymers no longer possess the rigidity necessary to produce the desirable mechanical properties.[4] Alternatively, sufficient solubility and lower melting point may be achieved by appending flexible side chains to rigid rod polymers. This third type of liquid-crystalline polymer has been the subject of a number of recent studies. Lenz and co-workers showed that substitution with linear or branched alkyl chains[5,6] considerably lowers the melting point of poly(phenylene terephthalate). Similar observations have been made in the course of a study of poly(3-*n*-alkyl-4-hydroxybenzoic acids).[7] Gray and co-workers demonstrated that side-chain-modified cellulose derivatives exhibit thermotropic as well as lyotropic behavior.[8,9] The solution properties of poly(γ-benzyl glutamates) (PBLG) are directly influenced by the presence of flexible side chains, as has been pointed out by Flory and Leonard.[10] The thermodynamics of PBLG in various solvents has been investigated theoretically as well as experimentally by Miller and co-workers,[11,12] leading to the conclusion

† Dedicated to the memory of Professor P. J. Flory.

0024-9297/86/2219-1366$01.50/0

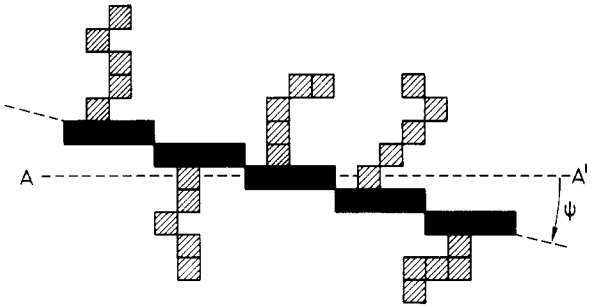

Figure 1. Representation of a rigid rod with appended side chains in a cubic lattice.

that the presence of flexible side chains in this polymer profoundly alters the phase diagrams as compared to the rigid rod model. In this work we present a comprehensive treatment of the thermodynamics of stiff rods with appended flexible side chains. As in the theory of Wee and Miller,[12] it is based on the lattice model originated by Flory,[13,14] which previously has been shown to account for all experimental facts obtained from suitable model systems.[15-19] Special attention is paid to the form of the orientational distribution function, as expressed in terms of the Flory–Ronca theory[20,21] or in the 1956 approximative treatment.[13] In order to treat lyotropic systems soft intermolecular forces are included by means of the familiar interaction parameter. Steric constraints between adjacent side chains appended to the same rod, an important problem in the course of a statistical-mechanical treatment of membranes[22] and semicrystalline polymers,[23] are not taken into account in the present treatment. It is assumed that the distances between neighboring side chains are sufficiently large, as is the case in the polyester systems mentioned above.[5,7] However, as discussed by Flory and Leonard,[10] this effect may come into play when helical polypeptides such as PBLG are considered.

Theory

The system considered here consists of rodlike molecules with flexible side chains appended regularly (cf. Figure 1).

As is customary, we subdivide the lattice into cells of linear dimensions equal to the diameter of the rodlike part of the particle. Thus the number of segments comprising this part is identical with its axial ratio, henceforth denoted by x. For simplicity, we take the segments of the side chains and the molecules of the solvent to be equal in size to a segment of the rodlike part. The axial ratio of the solvent therefore is given by $x_{solvent} = 1$. To each rod z side chains are appended comprising m segments. Since the side chains are not incorporated in the main chain, they are not expected to take part in the course of the ordering transitions. Therefore their configuration may be assumed to remain unaffected by the nature of the respective phase.

Consider a phase or liquid-crystalline domain where the rodlike parts of the molecules are preferentially oriented to the axis of the domain, the latter being taken along one of the principal axes of the lattice. As in ref 13, the stiff part consists of y sequences containing x/y segments (cf. Figure 1). The relation of y to the angle ψ of inclination to the axis of the domain will be discussed later in this section.

The calculation of the configurational partition function rests on the evaluation of the number ν_{j+1} of situations available to the $j + 1$ molecule after j particles are introduced. Let n_0 denote the total number of lattice sites and $f = x + mz$ the overall number of segments per molecule. Pursuant to the calculation of ν_{j+1}, it is expedient to introduce the rigid part first. Doing this we proceed along the lines given in ref 13. The number of situations available to the first segment of the first submolecule thus follows as the number of vacancies $n_0 - fj$. If there is no correlation between the adjacent rows parallel to the axis of the domain, the expectation of a vacancy required for the $y_{j+1} - 1$ first segments of the remaining submolecules is the volume fraction of the vacancies $(n_0 - fj)/n_0$. If a given site for the first segment of a submolecule is vacant, the site following it in the same row can then be only occupied by either the initial segment of a submolecule or a segment of a side chain. The conditional probability therefore is given by the ratio of vacancies to the sum of vacancies, submolecules, and total number of the segments of the side chains $(n_0 - fj)/(n_0 - fj + \sum^j y_i + zmj)$. Inasmuch as we assume that there is no correlation of the conformation of the side chains with the orientational order (see above), the expectancy of a vacancy for the zm segments of the side chains is given by the volume fraction of empty sites $(n_0 - fj)/n_0$. It follows that

$$\nu_{j+1} = (n_0 - fj) \times \left(\frac{n_0 - fj}{n_0}\right)^{y_{j+1}-1} \left(\frac{n_0 - fj}{n_0 - fj + \sum^{i} y_i + zmj}\right)^{x-y_{j+1}} \times \left(\frac{n_0 - fj}{n_0}\right)^{zm} \quad (1)$$

or

$$\nu_{j+1} = (n_0 - fj)^f (n_0 - xj + \sum^{j} y_i)^{y_{j+1}-x} {n_0}^{1-y_{j+1}-zm} \quad (2)$$

With negligible error we may write

$$\nu_{j+1} = \frac{(n_0 - fj)!}{n_0 - f(j+1)!} \frac{(n_0 - x(j+1) + \sum^{j+1} y_i)!}{(n_0 - xj + \sum^{j} y_i)!} {n_0}^{1-y_{j+1}-zm} \quad (3)$$

The results deduced by the lattice treatment are expected to become less secure at greater disorientations, i.e., at larger values of y/x. For the ordered phase under consideration here, this problem should be of minor importance, however. As usual,[20] the configurational partition function Z_M may be represented as the product of the combinatorial part Z_{comb}, the orientational part Z_{orient}, and the intramolecular or conformational part Z_{conf}:

$$Z_M = Z_{comb} Z_{orient} Z_{conf} \quad (4)$$

Since the configuration of the side chains is assumed to be independent of the order of the respective phase (see above), Z_{conf} may be dismissed in the subsequent treatment. The combinatorial part is related to ν_j by

$$Z_{comb} = \left(\frac{1}{n_x!}\right) \prod^{n_x} \nu_j \quad (5)$$

and thus follows as

$$Z_{comb} = \frac{(n_0 - n_x x + \bar{y} n_x)!}{n_x! n_1!} {n_0}^{n_x(1-\bar{y}-zm)} \quad (6)$$

where $n_1 = n_0 - fn_x$ denotes the number of solvent particles and n_x the number of polymer molecules. As usual, $\bar{y}$ is the average value of the disorder index y defined by

$$\bar{y} = \sum \frac{n_{xy}}{n_x} y \quad (7)$$

with n_{xy} being the number of molecules whose rigid core is characterized with regard to orientation by y. Following

Flory and Ronca,[20] the orientational part of Z_{orient} becomes

$$Z_{orient} = \prod_y \left(\frac{\sigma \omega_y n_x}{n_{xy}} \right)^{n_{xy}} \quad (8)$$

As in ref 20, ω_y denotes the a priori probability for the interval of orientation related to y, and σ is a constant. Introducing Stirling's approximation for the factorials, eq 4 together with eq 5 and 6 gives

$$-\ln Z_M = n_1 \ln v_1 + n_x \ln \frac{v_x}{x} - (n_0 - n_x x + \bar{y} n_x) \ln \left[1 - v_x \left(1 - \frac{\bar{y}}{x} \right) \right] - n_x (1 - \bar{y} - zm) + n_x \sum_y \frac{n_{xy}}{n_x} \ln \left[\frac{n_{xy}}{n_x} \frac{1}{\omega_y} \right] - n_x \ln \sigma \quad (9)$$

where the quantities $v_1 = n_1/n_0$ and $v_x = n_x x/n_0$ denote the volume fractions of the solvent and of the rigid core of the polymer, respectively.

For evaluating the orientational distribution we take the last molecule inserted into the lattice as a probe for the orientational order at equilibrium (see ref 20). Hence, equating $j + 1$ in eq 2 to n_x, we obtain

$$\nu_y \sim \left(1 - v_x \left(1 - \frac{\bar{y}}{x} \right) \right)^y \quad (10)$$

which immediately leads to

$$n_{xy}/n_x = f_1^{-1} \omega_y \exp(-ay) \quad (11)$$

with the quantity a defined by

$$a = -\ln \left[1 - v_x \left(1 - \frac{\bar{y}}{x} \right) \right] \quad (12)$$

and

$$f_1 = \sum_y \omega_y \exp(-ay) \quad (13)$$

Alternatively, eq 11 may be derived by variational methods.[20] Note that the orientational distribution function n_{xy}/n_x is given by the same expression as deduced in ref 20. Thus the functional dependence of n_{xy}/n_x on the disorientation index y of the rodlike part remains unaffected by the presence of flexible side chains. Accordingly, Z_{orient} follows as

$$Z_{orient} = n_x [\ln (f_1 \sigma) + a\bar{y}] \quad (14)$$

and, upon insertion into (9)

$$-\ln Z = n_1 \ln v_1 + n_x \ln \frac{v_x}{x} - (n_0 - n_x x) \ln \left[1 - v_x \left(1 - \frac{\bar{y}}{x} \right) \right] - n_x (1 - \bar{y} - zm) - n_x \ln (f_1 \sigma) \quad (15)$$

For examining the effect of small interactions between the solute particles, the heat of mixing ΔH_M is incorporated into the expression for the free energy. If it is assumed that randomness of mixing is preserved at all degrees of orientation, ΔH_M may be taken to be proportional to the number of segments of one type and the volume fraction of the other species. Hence, introducing the familiar interaction parameters χ_{12}, χ_{13}, and χ_{23}, ΔH_M becomes

$$\Delta H_M = \chi_{12} n_1 v_2 + \chi_{13} n_1 v_s + \chi_{23} n_2 v_3 \quad (16)$$

where the index 1 refers to the solvent, 2 to the rigid part of the solute particle, and 3 to the flexible side chains. The quantities χ_{ij} are given as usual[24] by

$$\chi_{ij} = Z_c \Delta w_{ij} x_j / RT \quad (17)$$

where x_j represents the number of segments per interacting species, Z_c is the coordination number, and Δw_{ij} ($=w_{ij} - 0.5(w_{ii} + w_{jj})$) denotes the change in energy for the formation of an unlike contact. Since the volume fraction v_s of the side chains depends on v_x through $v_s = v_x zm/x$, we have

$$\Delta H_M = \chi_1 n_1 v_x + \chi_2 n_x v_x \quad (18)$$

with

$$\chi_1 = \chi_{12} + \frac{zm}{x} \chi_{13} \quad (19)$$

and

$$\chi_2 = \frac{zm}{x} \chi_{23} \quad (20)$$

The chemical potentials are derived from eq 7 and 18 with the stipulation that at orientational equilibrium

$$\left(\frac{\ln Z_M}{(n_{xy}/n_x)} \right)_{n_1, n_x} = 0$$

Hence

$$\Delta\mu_1'/RT = \ln v_1 + v_s' + \frac{v_x'}{x}(y - 1) + a + v_x' \left[(v_x' + v_s')\chi_1 - \frac{v_x'}{x} \frac{zm}{x} \chi_2 \right] \quad (21)$$

and

$$\Delta\mu_x'/RT = \ln \frac{v_x'}{x} - f \left(v_1' + \frac{v_x'}{x} \right) + f - v_x' f \left(1 - \frac{\bar{y}}{x} \right) + zma - \ln (f_1 \sigma) + \left(1 - v_x' \frac{f}{x} \right) \left(v_1' x \chi_1 + v_x' \frac{zm}{x} \chi_2 \right) \quad (22)$$

In what is to follow all quantities referring to the anisotropic phase are marked by a prime. The corresponding expressions for the isotropic phase, obtained by equating y to x, are

$$\Delta\mu_1/RT = \ln v_1 + v_s + v_x \left(1 - \frac{1}{x} \right) + v_x \left[(v_x + v_s)\chi_1 - \frac{v_x}{x} \frac{zm}{x} \chi_2 \right] \quad (23)$$

$$\Delta\mu_x/RT = \ln \frac{v_x}{x} + f + f \left(v_1 + \frac{v_x}{x} \right) - \ln \sigma + \left(1 - v_x \frac{f}{x} \right) \left(v_1 x \chi_1 + v_x \frac{zm}{x} \chi_2 \right) \quad (24)$$

For evaluating the composition of the conjugated phases by means of the equilibrium conditions

$$\Delta\mu_1 = \Delta\mu_1' \quad (25)$$

$$\Delta\mu_2 = \Delta\mu_2' \quad (26)$$

the relation between y and the angle of inclination has to be specified. Since the orientational distribution as represented by eq 11 does not change when flexible side chains are appended to the stiff rods, we may directly use the expression given by the Flory–Ronca treatment of the lattice model.[20] Thus the disorder index y is represented by

$$y = \frac{4}{\pi} x \sin \psi \tag{27}$$

In orientational equilibrium its average value follows as

$$\bar{y} = \frac{4}{\pi} x f_2/f_1 \tag{28}$$

and the order parameter s becomes

$$s = 1 - {}^3/_2 f_3/f_1 \tag{29}$$

with the integrals f_p being given by

$$f_p = \int_0^{\pi/2} \sin^p \psi \exp(-\alpha \sin \psi)\, d\psi \tag{30}$$

The factor α relates to a (cf. eq 12) by

$$\alpha = \frac{4}{\pi} a x \tag{31}$$

For values of $\alpha \gg \pi/2$, the integrals f_p may be developed in series, yielding

$$f_1 = \frac{1}{\alpha^2} + \mathcal{O}\left(\frac{1}{\alpha^4}\right) \tag{32}$$

$$f_2 = \frac{2}{\alpha^3} + \mathcal{O}\left(\frac{1}{\alpha^5}\right) \tag{33}$$

$$f_3 = \frac{6}{\alpha^4} + \mathcal{O}\left(\frac{1}{\alpha^6}\right) \tag{34}$$

In this asymptotic approximation[20] the average disorder parameter $\bar{y}$ directly follows from

$$\bar{y} = \frac{2}{a} = -\frac{2}{\ln [1 - v_x(1 - \bar{y}/x)]} \tag{35}$$

Thus, we obtain for the chemical potentials eq 23 and 24 the expressions

$$\Delta\mu_1'/RT = \ln v_1' + v_s' + \frac{v_x'}{x}(\bar{y} - 1) + \frac{2}{\bar{y}} + v_x'\left[(v_x' + v_s')\chi_1 - \frac{v_x'}{x}\frac{zm}{x}\chi_2\right] \tag{36}$$

$$\Delta\mu_x'/RT = \ln \frac{v_x'}{x} - f\left(v_1' + \frac{v_x'}{x}\right) + f - v_x'\left(1 - \frac{\bar{y}}{x}\right) + \frac{2zm}{\bar{y}} + 2(1 - \ln \bar{y}) - \ln \frac{\sigma}{x^2} - C + \left(1 - v_x'\frac{f}{x}\right)\left[v_1' x \chi_1 + v_x'\frac{zm}{x}\chi_2\right] \tag{37}$$

where $C = 2 \ln (\pi e/8)$. Further simplification can be achieved by omitting the small constant C and equating σ to x (1956 approximation; cf. ref 11). In order to obtain the volume fraction of the polymer in the coexisting phases, trial values of v_x' and a (cf. eq 12) are chosen which serve for the numerical evaluation of the integrals f_p through eq 30. If the quantity α (eq 31) exceeds 30, the f_p may be calculated by the series expansion eq 32–34 using the first four terms. With the f_p being known, $\bar{y}$ follows from (28), which in turn leads to an improved value of a. The whole calculation is repeated until self-consistency is reached. Equation 26 is then solved numerically to obtain v_x, from which an improved value of v_x' is accessible via eq 25. The entire calculation is repeated with a new value of v_x' until compliance with all conditions for equilibrium is reached. When the 1956 approximation is used, the same scheme applies to eq 25 and 26, with eq 21 and 22 being replaced by eq 36 and 37. Here, self-consistency directly follows from eq 35. The volume fractions v_x' and v_x'' of two anisotropic phases in equilibrium can be evaluated by a similar numerical solution of (25) and (26) after insertion of (21) and (22) together with (28). Since this calculation is more sensitive toward the orientational distribution function, the exact treatment of Z_{orient} has to be used.

Results and Discussion

Parts a–d of Figure 2 show the phase diagrams resulting for rigid rods of axial ratio $x = 100$ with flexible side chains characterized by the number of side chains z per rod and the number of segments m per side chain.

From the theoretical treatment it is evident that only the product zm matters. Thus the polymer molecules under consideration here are fully determined by x and zm. Since the segments of the side chains are assumed to be isodiametric with the segments of the rigid core, the quantity zm/x directly gives the ratio of the volumes occupied by the respective parts of the molecule. For the present purpose of a discussion of the influence exerted by the side chains, the parameter χ_1 (see eq 19) measuring the interaction of the solvent and the rigid core will suffice to take into account intermolecular forces. The second parameter χ_2 related to the interactions of the side chains with the rigid core only matters at very high concentrations and is thus of minor importance.

Figure 2a corresponds to a system of rigid rods immersed in a solvent. The dashed lines indicate the metastable continuations of the phase lines. This diagram has been calculated by Flory in the famous work[13] in 1956 using the approximate form of the orientational distribution (see eq 36–38). The result given herein was obtained by resort to the treatment of the lattice model originated by Flory and Ronca.[20] A comparison of both methods shows that the main features of the diagram are rather insensitive toward the respective form of the orientational distribution function n_{xy}/n_x. However, the stability of the equilibria between two nematic phases is profoundly influenced by n_{xy}/n_x. This fact becomes even more important when going to lower axial ratios x. For example, the Flory–Ronca treatment predicts a triphasic equilibrium already for $x = 50$, an axial ratio not being sufficient to produce a stable nematic–nematic equilibrium in the frame of the 1956 approximation. From these results it is obvious that the exact treatment of n_{xy}/n_x is necessary for the precise calculation of the triphasic equilibria but is sufficiently accurate for evaluating the isotropic–nematic equilibrium at axial ratios greater than 100.

As can be seen from a comparison of Figure 2, part a, with parts b–d, there is a marked influence of the side chains on the phase behavior of rigid rods. We first discuss Figure 2, part a, 2a together with part b referring to $zm = 0$ and $zm = 2$, respectively. Here v_p and v_p' denote the total volume fractions of the polymer in the isotropic phase and in the coexisting ordered phase. Both phase diagrams exhibit the same gross features. At $\chi_1 = 0$ the soft interactions between the rods and the solvent are null, corresponding to athermal conditions. The narrow biphasic region at this point is continued until a pair of reentrant nematic phases appears at a critical point noted on the right-hand side of the ordinate. At a given value of χ_1, in the regime just beyond the critical point, either of two pairs of phases n,i or n,n may occur. Further increase of χ_1, equivalent to a lowering of temperature, leads to a triple point where three phases are in equilibrium. Raising χ_1 to still higher values is followed by a dilute isotropic phase in equilibrium with a dense nematic phase.

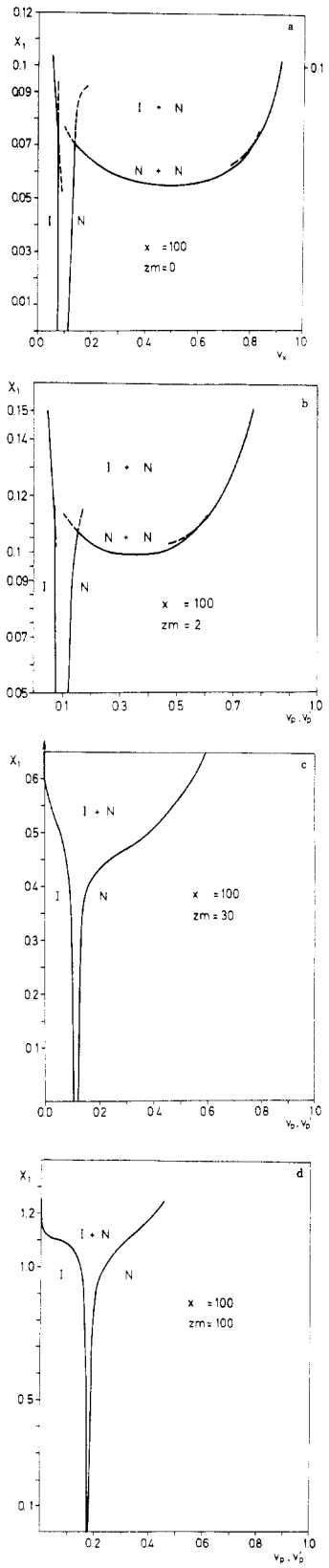

Figure 2. Phase diagrams of rigid rods immersed in a solvent; x is the axial ratio of the rigid core, z is the number of side chains per rigid core, and m is the number of segments per side chain. The solvent power is measured by the interaction parameter χ_1. The quantities v_p and v_x denote the volume fraction of the total polymer and its rigid core, respectively.

Several features command attention when Figure 2, parts a and b, are compared. Going from $zm = 0$ (perfectly rigid rods) to $zm = 2$ narrows considerably the region where to nematic phases are coexisting. If $zm > 4$, this region becomes unstable for $x = 100$. Note that both the critical value of χ_1 and its value at the triple point are increasing with appending of side chains. Furthermore, the anisotropic phase coexisting with the isotropic phase above the critical point is less concentrated when compared to $zm = 0$. Thus, even a small volume fraction of side chains as expressed by the ratio of zm to x suffices to change the phase behavior profoundly. This is even more obvious when higher values of zm (Figure 2c,d) are used. Here, the triphasic equilibrium is no longer stable. In addition, the widening of the biphasic gap occurs at much higher values of χ_1, as compared to rods without side chains (cf. Figure 2a; note the different scales of the ordinate in Figure 2a–d). Hence, the wide biphasic regime is expected to appear at a much lower temperature. Another feature of interest is the narrowing of the two-phase region with increase of zm at constant x. For athermal conditions this is shown in more detail in Figure 3a.

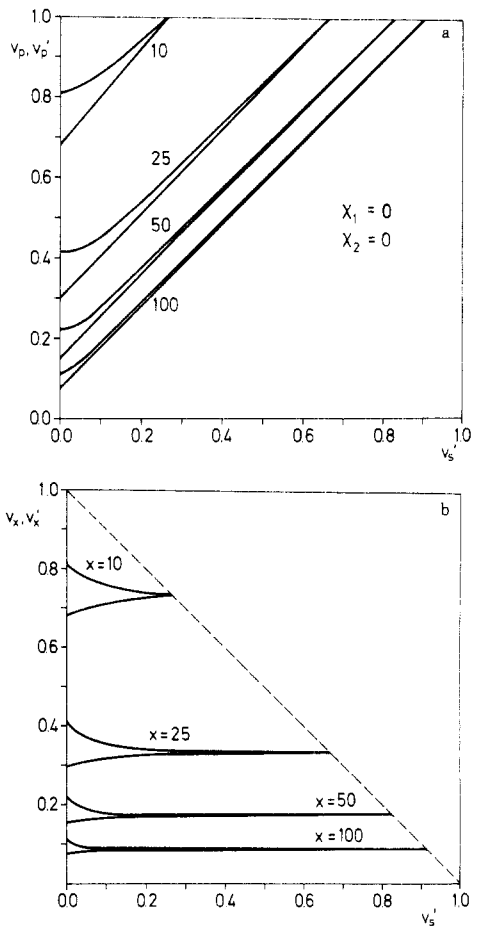

Figure 3. (a) Volume fraction v_p and v_p' of the polymer in the coexisting isotropic and anisotropic phase, respectively, at athermal conditions vs. the volume fraction v_s' of side chains in the anisotropic phase. (b) Volume fraction v_x and v_x' of the polymer in the coexisting isotropic and anisotropic phase, respectively, at athermal conditions vs. the volume fraction v_s' of side chains in the antisotropic phase.

Here the volume fractions v_p and v_p' in the respective phases are plotted against the volume fraction v_s' of the side chains in the anisotropic phase. It is evident that appending of even short chains results in a strong narrowing of the biphasic gap. This effect is most pronounced at higher axial ratios x where the two-phase region becomes negligible if $v_s' > v_x'$. Figure 3b shows the respective volume fractions v_x and v_x' of the rigid core of the polymer. As is obvious from this plot, the presence of flexible side chains changes the width of the biphasic gap but leaves the magnitude of v_x nearly unaffected. Clearly, as in Figure

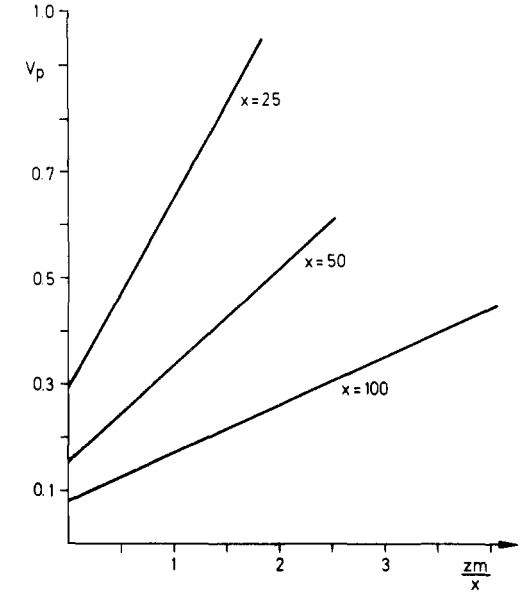

Figure 4. Volume fraction v_p of the polymer in the isotropic phase at equilibrium at athermal conditions vs. zm/x which gives the ratio of the volumes occupied by the side chains and the rigid core in the molecule, respectively.

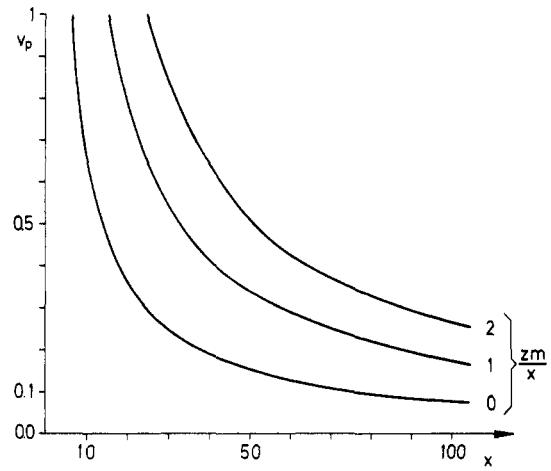

Figure 5. Volume fraction v_p of the polymer in the isotropic phase at equilibrium under athermal conditions vs. x, the axial ratio of the rigid core.

3a, the difference between v_x and v_x' is vanishing when $v_p = v_x + v_s$ is going to unity, i.e., when the whole system is filled with polymer. Since at athermal conditions v_x is nearly independent of zm, the total volume fraction of polymer v_p in the isotropic phase should increase linearly with zm. Figure 4 shows the dependence of v_p on $n(zm/x)$ to be linear indeed. It has to be noted that v_p must not be confused with v_p^*, the volume fraction for incipience of metastable order.[14] Thus, the ordering process among the rodlike cores is nearly unaffected by the presence of side chains, which appear to act like a low molecular weight solvent. This result clearly relates to the fact that one end of the flexible chain is fixed at the rigid core, which greatly reduces its entropy in solution. At higher polymer concentrations the number of configurations available to the side chains is becoming smaller. As a consequence of this unfavorable entropic effect, the concentration of the polymer in the anisotropic phase tends to smaller values at increasing values of zm. Since the isotropic phase is located at a more dilute regime, the overlap between the side chains should be smaller there. Hence, the volume fraction v_x of the rigid cores does not change very much upon appending of side chains. Consequently, the curves

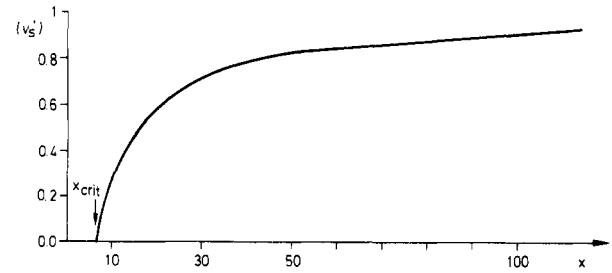

Figure 6. Maximum volume fraction of the side chains in the anisotropic phase at $v_p = 1$, i.e., in the neat liquid at athermal conditions. The quantity x_{crit} denotes the athermal limit being the minimum axial ratio to produce a stable nematic phase in the absence of attractive forces (cf. ref 20).

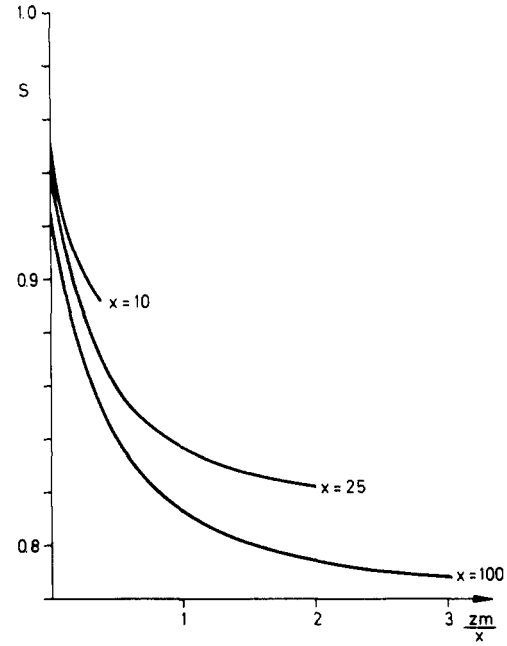

Figure 7. Order parameter s (cf. eq 29) at different axial ratios x of the rigid core vs. zm/x denoting the ratio of the volume occupied by the flexible side chains and the rigid core in the molecule, respectively.

describing the dependence of v_p on x are running nearly parallel to each other, the deviations at lower values of the axial ratio x notwithstanding (cf. Figure 5.) The situation, of course, is changed drastically if the side chains are allowed to move freely. As has been demonstrated by Flory,[25] this leads to a marked segregation of the rods and the random coils between the ordered and the isotropic phase.

As already discussed above, v_p reaches unity at a certain volume fraction of side chains $(v_s)^\infty$. This quantity, which may be taken as a measure of the maximum volume fraction to be tolerated by a nematic phase, is plotted against x in Figure 6. In the limit of high axial ratios x, $(v_s)^\infty$ tends to become unity. At low x $(v_s)^\infty$ is zero at $x_{crit} = 6.417$, which is the minimum axial ratio necessary for the occurrence of a nematic phase in the neat liquid.[20] In the vicinity of x_{crit} the dependence of $(v_s)^\infty$ on x is rather steep, indicating that an ordered phase composed of small rods can only tolerate a small volume fraction of side chains.

The foregoing considerations only hold true for athermal conditions. If χ_1 increases, the biphasic gap is widened, as is obvious from Figure 2b–d. Especially if zm is of the order of x, v_p becomes very small (cf. Figure 2d). However, the dense nematic phase at high values of χ_1 is less concentrated in the presence of side chains than compared to perfectly rigid rods. This is due to the entropic repulsion

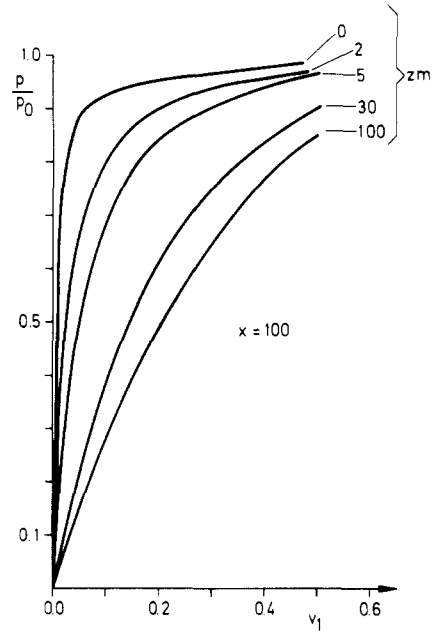

Figure 8. Reduced vapor pressure p/p_0 vs. volume fraction of solvent for an axial ratio of the rigid core $x = 100$. The quantity zm is the product of z, the number of side chains per rigid core, and m, the number of segments per side chains.

of the flexible side chains discussed above.

All results mentioned above suggest that the side chains may be compared to an ordinary solvent to a certain extent. However, as is demonstrated in Figure 7, the order parameter in the nematic phase (cf. eq 29) is lowered with increasing zm. Hence, as opposed to an ordinary solvent consisting of one segment, the flexible side chains interfere with the ordering process of the rodlike core.

Finally, we discuss the alterations effected by the presence of side chains at very high polymer concentrations. For this purpose the reduced vapor pressure p/p_0 of rods of axial ratio 100 with side chains characterized by zm is plotted vs. the volume fraction of solvent in Figure 8 (athermal conditions). The concentration range is restricted to those within in which the system is homogeneous, the single phase being anisotropic. Even at small ratios zm/x the resulting p/p_0 deviates strongly from its respective value at $zm = 0$. With zm of the order of x the reduced vapor pressure is fully governed by the side chains. If zm is becoming larger and larger ($zm > x$), the results of the present treatment coincide with those obtained by Flory and Leonard within the frame of their side-chain-mixing model.[10]

Having explored the various consequences of side chains on the ordering transition of rigid rods, we now turn to a comparison with experimental results. As pointed out in the beginning, stiff polyesters with appended flexible alkyl chains[5,7] seem to be the most promising systems for a quantitative test of the model developed herein. Unfortunately, the few data available on these polyesters only refer to the thermotropic behavior. At present, certain polypeptides exhibiting a stiff helical core in suitable solvents appear to be the best candidates for a test of theory. The cholesteric structure of these solutions does not hamper a comparison with theory since the pitch is much larger than typical molecular dimensions. To the author's knowledge Flory and Leonard[10] were the first to point out that the solution behavior of a number of helical polypeptides like poly(γ-benzyl glutamate) stems from the presence of flexible side chains. The thermodynamics of these polymers has been the subject of numerous studies since, especially by W. G. Miller and co-workers (ref 11, 12, 26, 27, and further literature cited therein). Presently, a number of excellent reviews on the subject are available.[11,28-31] Thus it suffices to focus only on the features relevant for the present purpose. For a comparison of theory with experimental data one has to bear in mind that the present model only treats molecularly uniform systems. However, the deviations due to the finite width of the distribution of chain length is expected to be of minor importance in the course of a more qualitative discussion.

In the phase diagrams predicted by theory three regions have to be distinguished: (1) the narrow biphasic region where χ_1 is small; (2) the small region in which two anisotropic phases may coexist; and (3) the wide biphasic regime at strong interactions between the rodlike cores.

Since the classical work of Robinson et al.[32] the point in region 1 where the polypeptide solution separates into two phases has been studied exhaustively (see the reviews on the subject, ref 11 and 28–32). This fraction v_p is accessible through optical[33] and viscometric[34] means. It has been used repeatedly for testing theoretical models (see, for instance ref 35). However, as has been revealed previously by the careful measurements of Sakamoto,[36] v_p in the isotropic phase strongly depends on solvent power. Due to aggregation PBGL ($M_w = 1.23 \times 10^5$) exhibits a v_p of 0.073 in chloroform, whereas dissolving the same polymer in DMF leads to $v_p = 0.124$. Recent measurements on light scattering by Schmidt[37] have demonstrated that DMF is a good solvent for PBGL. Thus aggregation, which clearly leads to a higher axial ratio, should be excluded under these conditions. However, even in DMF the volume fraction in the isotropic phase depends on temperature, as is obvious from the phase diagram given by Miller and co-workers.[11] This experimental finding, which may be due to the finite flexibility of the helical core,[37] makes a comparison of theory and experiment very difficult. A further problem encountered in the experimental investigation of the PBGL/DMF system is its extreme sensitivity toward small amounts of water[26] that can alter the phase behavior considerably. It is nevertheless interesting to compare the predictions for v_p by the rigid rod model[14] and the theory presented in this paper. Assuming a rodlike structure, Flory showed[14] that the axial ratios are obtained best from the densities of the respective polymers. Hence, according to this calculation a PBGL of molecular weight 2.20×10^5 (cf. Table 2 of ref 14) may be characterized by an axial ratio x of 97. From this value of x the volume fraction v_p in the isotropic phase is given by 0.078. Assuming that the volume of the solid polymer consists of equal parts of rigid core and side chains ($zm/x = 1$) leads to an increase of x by a factor of $2^{1/2}$; i.e., the axial ratio of 137 thus calculated is followed by $v_p = 0.1322$. The present data[11] suggest a ratio zm/x smaller than 1, but the temperature dependence of v_p exhibited by PBGL/DMF and poly[(carbobenzoxy)lysine]/DMF[11] does not allow a more quantitative conclusion at the present stage. However, both systems reveal a biphasic gap in region 1 much smaller than that calculated from the rigid rod model.[11] Thus the prediction of a narrowing of the two-phase region (cf. Figure 2a–d) is substantiated by experimental findings.

If the solvent power is slightly deteriorated, the rigid rod model predicts the occurrence of two anisotropic phases in equilibrium (see Figure 2a). In the presence of side chains the interaction parameter χ_1 at the point where the systems enters region 2 is shifted to much higher values (cf. Figure 2b). If zm/x exceeds a certain critical value for a given axial ratio, region 2 is predicted to vanish. The experimental investigation of this region is particularly

difficult. In most solvents gelation will occur[28,38] upon lowering of the temperature, which clearly demonstrates the strong interactions between the particles. Even in good solvents, extreme care has to be taken in order to avoid the occurrence of a "complex phase" due to traces of water.[26] Nakajima, Hayashi, and Ohmori[39] have given evidence for a triphasic equilibrium in the system PBGL/DMF/methanol. Recently, Russo and Miller[27] investigated this feature in great detail. From their measurements they concluded that PBGL/DMF exhibits an equilibrium of two anisotropic phases, whereas poly[(carbobenzoxy)lysine]/DMF does not show any evidence of such a phenomenon. For comparison of theory and experiment one has to bear in mind that the rigid rod model predicts region 2 to appear at small positive values of χ_1. Measurements of the solvent activities by Kubo and Ogino,[40] however, inevitably lead to the conclusion that the small biphasic region 1 is extended to much lower solvent power. Another feature important for the discussion of this point is the conformation of the side chains, which has been the subject of a number of recent studies by NMR[41-43] and by measurements of the magnetic susceptibility.[44] The results obtained by these investigations, especially the work by Toriumi, Matsuzawa, and Uematsu,[44] demonstrate a finite stiffness of the side chains. Consequently, in the concentration regime under consideration here there is a finite order parameter of this moiety (ca. 0.1) which decreases with increasing temperature.[44] Hence, a part of the side chains enlarges the rigid core, leading to a lower value of the ratio of zm to x. Similar conclusions may be drawn from the comparatively small values of v_p in region 1 (see above). Thus, these experimental findings are indicative of an increasing stiffness of the side chains in PBLG with ascending concentration. However, the system poly[(carbobenzoxy)lysine]/DMF,[11] in which the side chains are longer than in PBGL, does not show any evidence of a nematic–nematic equilibrium, in accord with the theory presented herein.

Only a few data are available for a discussion of region 3, the wide biphasic gap. In most cases studied so far,[28] the solutions form a mechanically self-supporting gel when brought to temperatures near this regime. This, of course, is in accord with theory, which predicts the widening of the two-phase region at a much lower solvent power as compared to systems consisting of perfectly rigid rods. Thus gelation may interfere with the ordering process. At the lowest temperatures accessible for PCBL/DMF only a minute enlargement of the biphasic gap is observed.[11] In PBGL/DMF the existing data on region 3[11] show the volume fraction of the dense nematic phase to be smaller than that calculated from the rigid rod model[11] but wider than expected from the treatment given in this paper. This again may be due to alterations of the conformation of the side chains discussed above.

A further aspect of lyotropic solutions that merits attention is the degree of order in the nematic phase. The lattice theory of rigid rods[14] as well as the theory given herein makes explicit predictions in this regard in terms of the disorder index y (eq 7) and the familiar order parameter s (eq 29). Although the latter quantity has been exhaustively studied in low molecular weight nematogens, it has been largely ignored in investigations of lyotropic polymer solutions. The data given by Samulski and coworkers[30] on PBGL in dioxane show s to be of the order of 0.5 at the transition point. At higher concentration a value of approximately 0.7–0.8 results, in better agreement with the data presented in Figure 7. Clearly, a more detailed investigation of s as function of concentration, temperature, and molecular weight will clarify this point.

Conclusions

It has been shown that the Flory lattice model can be modified easily to take into account the presence of flexible side chains. The resulting phase diagrams are in qualitative agreement with experimental data of lyotropic solutions of helical polypeptides. However, the effect of special inter- and intramolecular interactions among the side chains, as evident in solutions of PBGL, needs further exploration, preferably by NMR techniques.[45] Also, results obtained on systems with varying lengths of side chains[46] will clearly lead to a more conclusive test of the theory presented in this paper.

Acknowledgment. The author is indebted to the late Prof. P. J. Flory for helpful discussions and encouragement.

References and Notes

(1) Prevorsek, D. C. In *Polymer Liquid Crystals* Cifferi, A., Krigbaum, W. R., Meyer, R. B., Eds.; Academic: New York, 1982.
(2) Jackson, W. J. *Br. Polym. J.* **1980**, *12*, 154.
(3) Ober, Ch. K.; Jin, J.-I.; Lenz, R. W. *Adv. Polym. Sci.* **1984**, *59*, 103.
(4) Krigbaum, W. R.; Cifferi, A.; Acierno, D. *J. Appl. Polym. Sci., Appl. Polym. Symp.* **1985**, *41*, 293.
(5) Majnusz, J.; Catala, J. M.; Lenz, R. W. *Eur. Polym. J.* **1983**, *19*, 1043.
(6) Dicke, H.-R.; Lenz, R. W. *J. Polym. Sci., Polym. Chem. Ed.* **1983**, *21*, 2581.
(7) Ballauff, M.; Stern, R.; Wegner, G., unpublished data.
(8) Tseng, S. L.; Laivins, G. V.; Gray, D. G. *Macromolecules* **1982**, *15*, 1262.
(9) Laivins, G. V.; Gray, D. G. *Macromolecules* **1985**, *18*, 1753.
(10) Flory, P. J.; Leonard, W. J., Jr. *J. Am. Chem. Soc.* **1965**, *87*, 2102.
(11) Miller, W. G.; Wu, C. C.; Wee, E. L.; Santee, G. L.; Rai, Y.; Goebel, K. G. *Pure Appl. Chem.* **1974**, *38*, 37.
(12) Wee, E. L.; Miller, W. G. *Liq. Cryst. Ordered Fluids* **1978**, *3*, 371.
(13) Flory, P. J. *Proc. R. Soc. London, A* **1956**, *73*, 234.
(14) Flory, P. J. *Adv. Polym. Sci.* **1984**, *59*, 1.
(15) Irvine, P. A.; Flory, P. J. Wu, Dacheng *J. Chem. Soc., Faraday Trans. 1* **1984**, *80*, 1795.
(16) Flory, P. J.; Irvine, P. A. *J. Chem. Soc., Faraday Trans. 1* **1984**, *80*, 1807.
(17) Irvine, P. A.; Flory, P. J. *J. Chem. Soc., Faraday Trans. 1* **1984**, *80*, 1821.
(18) Ballauff, M.; Wu, Dacheng; Flory, P. J.; Barrall, E. M., II *Ber. Bunsen-Ges. Phys. Chem.* **1984**, *88*, 524.
(19) Ballauff, M.; Flory, P. J. *Ber. Bunsen-Ges. Phys. Chem.* **1984**, *88*, 530.
(20) Flory, P. J.; Ronca, G. *Mol. Cryst. Liq. Cryst.* **1979**, *54*, 289.
(21) Flory, P. J.; Ronca, G.; *Mol. Cryst. Liq. Cryst.* **1979**, *54*, 311.
(22) Dill, K. A.; Flory, P. J. *Proc. Natl. Acad. Sci. U.S.A. 77*, **1980**, 3115.
(23) Flory, P. J.; Yoon, D. Y.; Dill, K. A. *Macromolecules* **1984**, *17*, 862.
(24) Flory, P. J. *Principles of Polymer Chemistry*; Cornell University: Ithaca, NY, 1953.
(25) Flory, P. J. *Macromolecules* **1978**, *11*, 1138.
(26) Russo, P. S.; Miller, W. G. *Macromolecules* **1984**, *17*, 1324.
(27) Russo, P. S.; Miller, W. G. *Macromolecules* **1983**, *16*, 1690.
(28) Uematsu, I.; Uematsu, Y. *Adv. Polym. Sci.* **1984**, *59*, 37.
(29) DuPre, D. B.; Samulski, E. T. In *Liquid Crystals, The Fourth State of Matter*; Saeva, F. D., Ed.; Dekker: New York, 1979.
(30) Samulski, E. T. In *Liquid Crystalline Order in Polymers*; Blumstein, A., Ed.; New York, 1978.
(31) Iizuka, E. *Adv. Polym. Sci.* **1976**, *20*, 79.
(32) Robinson, C.; Ward, I. C.; Beevers, R. B. *Discuss. Faraday Soc.* **1958**, *25*, 29.
(33) Toyoshima, Y.; Minami, N.; Sukigara, M. *Mol. Cryst. Liq. Cryst.* **1976**, *35*, 325.
(34) Hermans, J., Jr. *J. Colloid Sci.* **1962**, *17*, 638.
(35) Straley, J. P. *Mol. Cryst. Liq. Cryst.* **1973**, *22*, 333.
(36) Sakamoto, R. *Colloid Polym. Sci.* **1984**, *262*, 788.
(37) Schmidt, M. *Macromolecules* **1984**, *17*, 553.
(38) Sasaki, S.; Tokama, K.; Uematsu, I. *Polym. Bull. (Berlin)* **1983**, *10*, 539.

(39) Nakajima, A.; Hayashi, T.; Ohmori, M. *Biopolymers* **1968**, *6*, 973.
(40) Kubo, K.; Ogino, K. *Polymer* **1975**, *16*, 629.
(41) Rai, J. W.; Miller, W. G.; Bryant, R. G. *Macromolecules* **1973**, *6*, 262.
(42) Shoij, A.; Ozaki, T.; Saito, H.; Tabeta, R.; Ando, I. *Macromolecules* **1984**, *17*, 1472.
(43) Czarniecka, K.; Samulski, E. T. *Mol. Cryst. Liq. Cryst.* **1981**, *63*, 205.
(44) Toriumi, H.; Matsuzama, K.; Uematsu, I. *J. Chem. Phys.* **1984**, *81*, 6085.
(45) Spiess, H. W. *Adv. Polym. Sci.* **1985**, *66*, 24.
(46) Hanabusa, H.; Sato, M.; Shirai, H.; Takemoto, K.; Iizuka, E. *J. Polym. Sci., Polym. Lett. Ed.* **1984**, *22*, 559.

Interactions between Surfaces with Adsorbed Polymers: Poor Solvent. 2. Calculations and Comparison with Experiment

Kevin Ingersent,† Jacob Klein,* and Philip Pincus‡

Magdalene College, Cambridge, England, Cavendish Laboratory, Cambridge, England, and Polymer Department, Weizmann Institute of Science, Rehovot 76 100, Israel, and Corporate Laboratories, Exxon Research, Clinton Township, Annandale, New Jersey 08801.
Received September 16, 1985

ABSTRACT: Analytical expressions, based on a mean-field model and derived in a previous paper (part 1: Klein, J.; Pincus, P. A. *Macromolecules* **1982**, *15*, 1129), for the interaction between two parallel plates bearing adsorbed polymer in poor-solvent medium, are solved numerically to yield (a) segmental density profiles of the adsorbed polymer and (b) interaction-energy vs. plate-separation profiles. All parameters appearing in these calculations are obtainable from bulk data such as the polymer–solvent phase diagram and adsorbance measurements. The calculated results are critically compared with model experiments on forces between smooth mica surfaces bearing polystyrene in cyclohexane in poor-solvent conditions: the agreement is qualitatively very good and quantitatively fair. Some improvements to the model are suggested.

I. Introduction

It has long been known that layers of flexible polymers adsorbed at solid–liquid interfaces may strongly modify the surface–surface forces; this effect is commonly used to stabilize (or destabilize) colloidal dispersions and is also encountered in many naturally occurring biocolloidal systems. The experimental and theoretical situation up to about 1981 has been comprehensively reviewed by Vincent[1] and by Vincent and Whittington.[2]

Theoretical treatment of the problem of interaction between surfaces bearing adsorbed polymer layers is complicated by the number of effects that may contribute; these include osmotic interactions between opposing adsorbed segments, volume-exclusion effects due to the impermeable walls, and the sticking energy of segments adsorbed on the solid surface. It may also be possible for single molecules to span the interplate gap, and such bridging always leads to attraction. In addition, any theoretical models must make assumptions about the state of equilibrium of the adsorbed polymer layers when they are moved relative to each other; as surface diffusion phenomena are often very slow, such assumptions require great care.

Over the past few years there have been a number of model experimental studies of the interaction between atomically smooth solid (mica) surfaces bearing adsorbed polymer layers and immersed in liquid media in a variety of solvency conditions.[3-6] These studies are sufficiently direct to invite quantitative comparison between the experimental results and the predictions of theoretical models; in this way we may hope to get insight into the ways in which such models may be improved and also into the validity of the assumptions (such as state of equilibrium) made in such comparisons.

Recent attempts at analysis have fallen into two broad categories. Scheutjens and Fleer[7] have applied the transfer matrix techniques of Rubin[8] and DiMarzio,[9] and their treatment accounts for the possible chain conformations, suitable weighted on a quasi-crystalline lattice. In the Cahn–de Gennes approach[10-12] one minimizes the excess free energy of the adsorbed interacting polymer layers with respect to the segmental density profile $\phi(z)$ at distance z from each surface; de Gennes used this approach to calculate the interaction–distance profile between adsorbed polymer layers in a good-solvent system, using scaling exponents to go beyond Flory–Huggins mean-field theory.[12] In an earlier paper,[13] hereafter referred to as part 1, Klein and Pincus extended de Gennes' treatment[12] to calculate the interaction between irreversibly adsorbed polymer layers below the Θ-point, where Flory–Huggins mean field is a good approximation.[14,15] The assumption of irreversible adsorption is suggested by experiment[3] and reflects the fact that even when the sticking energy per monomer is small, the total sticking energy per polymer molecule may greatly exceed its thermal energy k_BT. Under these poor-solvent conditions an attractive interaction was predicted[13] at plate separations greater than about R_g (the unperturbed radius of gyration of the polymer) and repulsive forces for narrow gaps. This agreed qualitatively with the results of direct force measurements between polystyrene (PS) layers adsorbed on mica surfaces in cyclohexane (CH). We have now used computational methods to obtain force profiles which can be compared quantitatively with experiment.

In the next section there is a summary of the mean-field theory from part 1, leading to coupled integral equations that determine the interfacial energy. The set of coupled equations is solved numerically, as briefly described in section III, and the results are presented in section IV. In section V these predictions are compared critically with

* Cavendish Laboratory and Weizmann Institute of Science. Address correspondence to the Weizmann Institute.
† Magdalene College. Present address: Department of Physics, University of Pennsylvania, Philadelphia, PA.
‡ Exxon Research. Present address: Department of Chemical Engineering, University of California at Santa Barbara, Santa Barbara, CA 93106.

0024-9297/86/2219-1374$01.50/0